Nuclear magnetic resonance of ^{209}Bi in a $BiVO_4$ single crystal

1992 J. Phys.: Condens. Matter 4 1607

(http://iopscience.iop.org/0953-8984/4/6/026)

J. Phys.: Condens. Matter 4 (1992) 1607–1613. Printed in the UK

Nuclear magnetic resonance of ^{209}Bi in a $BiVO_4$ single crystal

A R Lim†‡, S H Choh† and M S Jang§

† Department of Physics, Korea University, Seoul 136–701, South Korea

§ Department of Physics, Pusan National University, Pusan 609–735, South Korea

Received 15 August 1991, in final form 22 October 1991

Abstract. Nuclear magnetic resonance spectra of ^{209}Bi ($I = \frac{9}{2}$) in the ferroelastic $BiVO_4$ single crystal has been investigated by employing a wide-line Varian spectrometer. Only three lines due to a large quadrupole interaction were measured at a fixed frequency of 6 MHz in the principal planes at room temperature. From the experimental data the quadrupole coupling constant $e^2qQ/h = 79.2 \pm 0.1$ MHz and asymmetry parameter $\eta = 0.70 \pm 0.01$ are determined; however, these values turn out to be quite different from the previous report obtained with a ceramic sample at liquid-nitrogen temperature. The principal axes of the electric field gradient tensor are determined for the first time, the x, y and z axes being the crystallographic $c + 25°$, $a + 25°$, and b axes, respectively. These directions are discussed in terms of the Bi–O bonds in the Bi–O polyhedra.

1. Introduction

Bismuth vanadate ($BiVO_4$) has received considerable attention since the discovery of a ferroelastic–paraelastic phase transition at 528 K by Bierlein and Sleight (1975). The transition is from a tetragonal scheelite structure (space group, $I4_1/a$) to a low-temperature monoclinic system (space group, $I2/a$). Recently, there have been a great deal of experimental investigations such as x-ray diffraction (David *et al* 1979), neutron diffraction (Sleight *et al* 1979), Raman scattering (Pinczuk *et al* 1979, Jang *et al* 1985), and NMR (Choh *et al* 1985, Moon *et al* 1987, Lim *et al* 1989a), to study the structural changes and the phase transition.

In this paper we present the ^{209}Bi NMR of the ferroelastic phase of $BiVO_4$ single crystals grown by the Czochralski method. The quadrupole coupling constant, the asymmetry parameter and the direction of the principal axes of the electric field gradient tensor (EFG) of ^{209}Bi ($I = \frac{9}{2}$) are determined at room temperature. It appears that this is the first report of ^{209}Bi NMR in the single-crystal form of $BiVO_4$. The preliminary result was orally presented at a Korean Physical Society Meeting (Lim *et al* 1989b).

2. Crystal structure

The ferroelastic $BiVO_4$ crystal is known to undergo a reversible second-order phase transition at T_c between the ferroelastic monoclinic and the paraelastic tetragonal

‡ Present address: Magnetics Laboratory, Korea Standards Research Institute, Taejeon 305–606, South Korea.

0953-8984/92/061607 + 07 $04.50

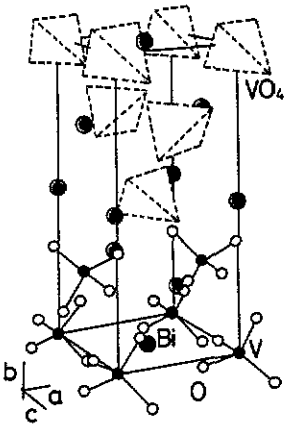

Figure 1. The paraelastic tetragonal structure of $BiVO_4$ (scheelite structure).

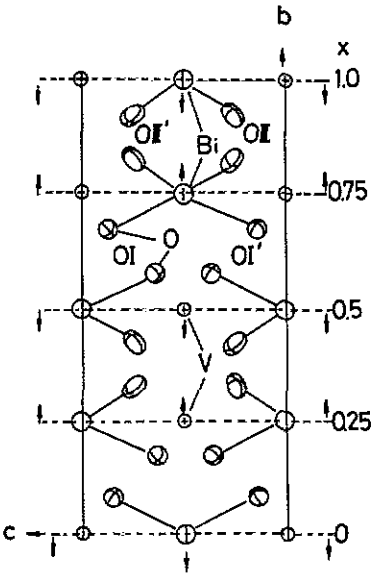

Figure 2. The structure of $BiVO_4$ projected on the $(00\bar{1})$ plane. Atomic displacements along [010] and $[0\bar{1}0]$ are shown in the ferroelastic phase.

structure (Dudnik *et al* 1979). The ferroelastic phase of $BiVO_4$ has the point group $2/m$ with lattice constants $a = 5.1966$ Å, $b = 11.704$ Å, $c = 5.0921$ Å and $\beta = 90.384°$ at room temperature. The scheelite structure of $BiVO_4$ is shown in figure 1. The monoclinic phase has distortions from the scheelite structure due to small displacements of Bi^{3+} and V^{5+} cations along the b axis, as shown by arrows in figure 2 (Sleight *et al* 1979). The vanadium atom is in an isolated oxygen tetrahedron and the bismuth atom is coordinated by eight isolated tetrahedra.

3. Experimental procedure

The equipment used for NMR measurements is a Varian model WL-112 wide-line spectrometer, the same as previously described (Lim *et al* 1989a). The $BiVO_4$ single crystals were grown by melting a mixture of Bi_2O_3 (purity 99.9%) and V_2O_5 (purity 99.9%) powder. The orientation of the specimen was determined by the x-ray Laue method. All NMR data were obtained at a fixed frequency of 6 MHz at room temperature.

The ^{209}Bi (100% natural abundance) nucleus has the nuclear spin $I = \frac{9}{2}$ which may lead to nine allowed NMR transitions. However, as a result of the large quadrupole interaction and wide linewidths (7–9 mT), the detected signals were very weak, and the signal-to-noise ratio was only 3 to 1 as shown in figure 3. The employed sample crystal dimension was approximately 13 mm diameter and 10 mm long.

4. Experimental data and analysis

The rotation patterns of ^{209}Bi NMR spectra measured in the principal planes are displayed in figures 4 and 5. The points are the data and the curves represent calculations discussed later.

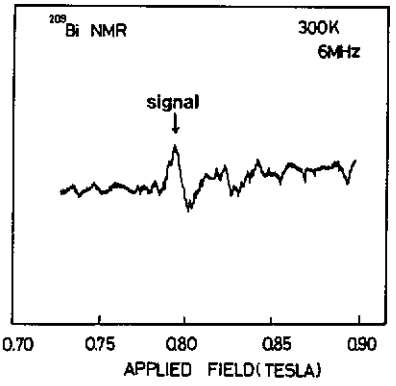

Figure 3. A typical NMR signal of ^{209}Bi in $BiVO_4$, marked with an arrow, obtained with B parallel to the a axis.

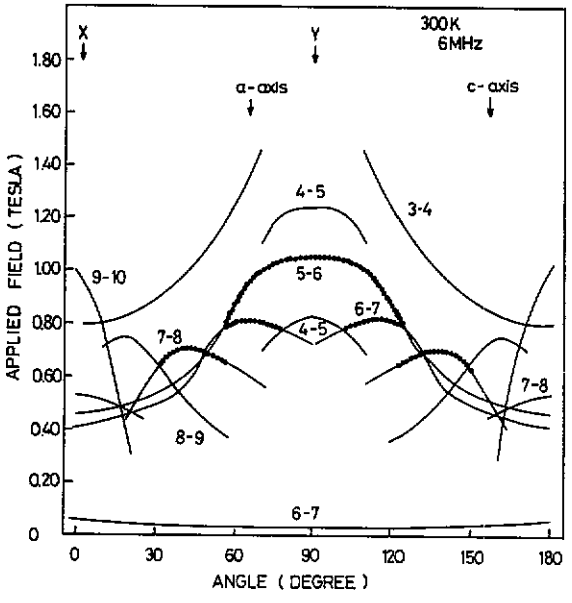

Figure 4. Rotation pattern of ^{209}Bi NMR in the crystallographic a–c plane at 300 K.

The Hamiltonian to analyse these results is as usual

$$H = H_Z + H_Q \tag{1}$$

where H_Z is the Zeeman term and H_Q describes the nuclear electric quadrupole interaction of the ^{209}Bi ($I = \frac{9}{2}$) nucleus. The quadrupole Hamiltonian in the principal axes system of the EFG tensor is given by

$$H_Q = e^2qQ[3I_z^2 - I(I+I) + \tfrac{1}{2}\eta(I_+^2 + I_-^2)]/4I(2I-1) \tag{2}$$

where e^2qQ/h is the quadrupole coupling constant and η is the asymmetry parameter. Conventionally the x, y and z axes are such that $|V_{xx}| \leqslant |V_{yy}| \leqslant |V_{zz}| = eq$; then

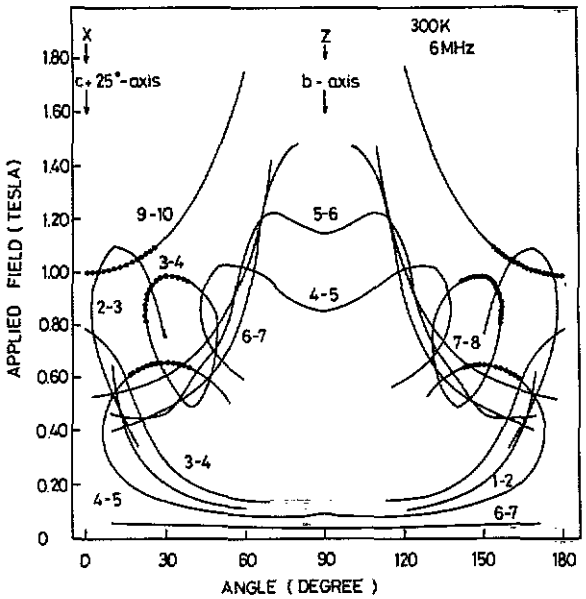

Figure 5. Rotation pattern of ^{209}Bi NMR in the c'–b plane at 300 K, where c' is the axis tilted 25° from the c axis in the c–a plane.

$0 \leqslant \eta \leqslant 1$. The matrix form of the spin Hamiltonian of equation (1) is employed to calculate the resonance points with the magnetic field applied along a general direction. All resonance spectra and the parameters are calculated by numerically diagonalizing the matrix using a computer program with the experimental data.

5. Results

In general the rotation patterns in three mutually perpendicular planes are required to determine the quadrupole interaction completely. The rotation pattern measured in a crystallographic plane turned out to be not the principal plane of the EFG tensor, as shown in figure 4, and figure 5 was obtained after a preliminary analysis.

The maximum separation due to the quadrupole interaction was observed when the magnetic field was applied along the b axis of the crystal and this direction is analysed to be the z axis of the EFG tensor. Accordingly, the quadrupole parameters are determined by the least-squares fit with the experimental data in figures 4 and 5. Labels near each line refer to the pairs of energy levels involved in the transitions; the larger the number, the higher is the level, and line 5–6 is the central transition. We were unable to detect the ^{209}Bi signals in the range from 0.4 to 0.6 T, where the ^{51}V signals were recorded with a much stronger intensity.

From the experimental data, the quadrupole coupling constant $e^2qQ/h = 79.2 \pm 0.1$ MHz and the asymmetry parameter $\eta = 0.70 \pm 0.01$ at room temperature are determined. However, these values turn out to be quite different from those in the previous report (Volkov *et al* 1978), obtained with a ceramic sample at liquid-nitrogen

Table 1. Quadrupole parameters of ^{209}Bi in $BiVO_4$.

Sample	e^2qQ/h (MHz)	η	Principal axes	Temperature (K)	References
Single crystal	79.2 ± 0.1	0.70 ± 0.01	$x = c + 25°$ $y = a + 25°$ $z = b$	300	Present work
Ceramic	149 ± 5	0.9 ± 0.1		77	Volkov *et al*

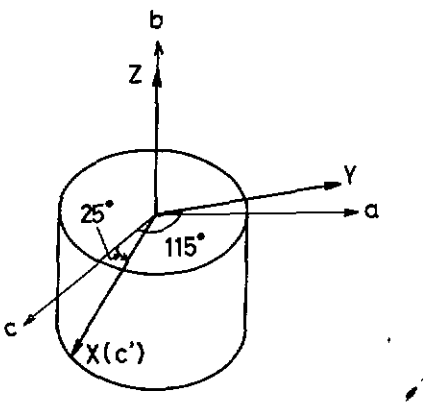

Figure 6. The relation between the principal axes of the EFG tensor of ^{209}Bi and the crystallographic axes of $BiVO_4$. The x and y axes are in the c–a plane.

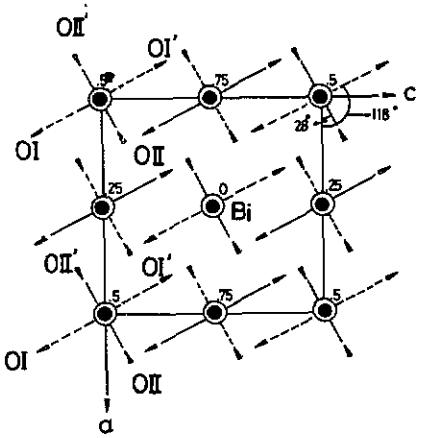

Figure 7. Projection on the (010) plane of the $BiVO_4$ structure.

temperature. The analysed parameters of the ^{209}Bi nucleus are summarized in table 1 together with the previous report. The principal x, y and z axes of the EFG tensor of the Bi ion in the ferroelastic phase are found to be along the crystallographic $c + 25°$, $a + 25°$ and b axes, respectively. The relation between the principal axes of the EFG tensor and the crystallographic axes is shown in figure 6.

6. Discussion

While the principal axes of the EFG tensor of the V ion in the ferroelastic phase of $BiVO_4$ were found to be along the crystallographic axes ($x = c$, $y = a$ and $z = b$), instead of the V–O bond axes of the VO_4 tetrahedron, as reported previously (Choh *et al* 1985, Lim *et al* 1989a), the principal x, y and z axes of the EFG tensor of the Bi ion in the ferroelastic phase are found to be along the $c + 25°$, $a + 25°$ and b axes, respectively. The principal axes systems of EFG tensors of ^{51}V and ^{209}Bi are, however, simply related; the z axis is the same along the b axis and the x and y axes for ^{209}Bi are rotated by 25° along the b axis.

In order to comprehend the principal axes of the EFG tensor, we have attempted a simple approach due to David and Wood (1983) that ascribes the structural analysis

Table 2. The bond lengths and bond strengths of the monoclinic $BiVO_4$ at 300 K.

Bond type	Bond length (Å)	Bond strength
Bi–O(I)	2.502	0.334
Bi–O(I′)	2.640	0.256
Bi–O(II)	2.379	0.431
Bi–O(II′)	2.343	0.464
V–O(I)	1.694	1.329
V–O(I′)	1.694	1.329
V–O(II)	1.769	1.066
V–O(II′)	1.769	1.066

Table 3. The fractional differences in bond lengths and bond strengths.

Bond type	l_1	s_1	l_2	s_2	$\lvert(l_1 - l_2)/(l_1 + l_2)\rvert$ (%)	$\lvert(s_1 - s_2)/(s_1 + s_2)\rvert$ (%)
Bi–O	2.502	0.334	2.379	0.431	2.52	12.6
Bi–O′	2.640	0.256	2.343	0.464	5.97	28.9
V–O	1.694	1.329	1.769	1.066	2.16	11.0
V–O′	1.694	1.329	1.769	1.769	2.16	11.0

of the ferroelastic distortion in $BiVO_4$ using the bond length versus bond strength relationship. The Bi–O and V–O bond lengths and their accompanying bond strengths, for $BiVO_4$ at 300 K, are presented in table 2. Also shown in table 3 are the fractional differences in bond lengths and bond strengths. Although there are changes in all bond strengths, the most significant change is that associated with one of the Bi–O bonds, which has a fractional change approaching 30%. Therefore, the Bi–O interaction appears to contribute more to the ferroelastic distortion than does the V–O interaction. In addition, the oxygen ions must be taken into account as bridges in a Bi–O–V system, with an effective transfer of charge to and from the Bi–O and V–O bonds. Accordingly the geometric angles of the Bi–O(I) bonds and Bi–O(II) bonds in the Bi–O polyhedra, approximately 28° and 118° to the a axis (David and Wood 1983) as shown in figure 7 are considered. These directions are reasonably close to $y = a + 25°$ and $x = c + 25°$, respectively, in the a–c plane. This is consistent with the fact that B–O(II) bonds are shorter than B–O(I) bonds while the components of the EFG tensor are such that $|V_{xx}| < |V_{yy}|$ with $\eta \neq 0$. The z axis along the b axis is, however, not immediately obvious from the crystal structure. The z axis of the EFG tensors of ^{51}V and ^{209}Bi in $BiVO_4$ are all along the b axis. These results may be related to the fact that the ferroelastic distortions are displacements of V^{5+} and Bi^{3+} cations along the b axis, where the EFG component is the strongest.

Acknowledgment

We acknowledge gratefully the financial support of the Basic Science Research Institute Program of the Ministry of Education (1989–94).

References

Bierlein J D and Sleight A W 1975 *Solid State Commun.* **16** 69
Choh S H, Moon E Y, Park Y H and Jang M S 1985 *Japan. J. Appl. Phys.* 2 **24** 640
David W I F, Glazer A M and Hewat A W 1979 *Phase Trans.* **1** 155
David W I F and Wood I G 1983 *J. Phys. C: Solid State Phys.* **16** 5093
Dudnik E P, Gene B B and Mnushkina I E 1979 *Bull. Acad. Sci. USSR, Phys. Ser.* **43** 149
Jang M S, Park H L, Kim J N, Ro J H and Park Y H 1985 *Japan. J. Appl. Phys.* 2 **24** 506
Lim A R, Choh S H and Jang M S 1989a *Ferroelectrics* **94** 389
—— 1989b *Bull. Korean Phys. Soc.* **7** 227
Moon E Y, Choh S H, Park Y H, Yeom H Y and Jang M S 1987 *J. Phys. C: Solid State Phys.* **20** 1867
Pinczuk A, Burns G and Dacol F H 1979 *Solid State Commun.* **29** 515
Sleight A W, Chen H Y, Ferretti A and Cox D E 1979 *Mater. Res. Bull.* **14** 1571
Volkov A F, Ivanova L A and Venevtsev Y N 1978 *Sov. Phys.–Solid State* **14** 617